ELSEVIER

Cement and Concrete Composites **20** (1998) 393–404
0958-9465/98/$ — see front matter

PII:S0958-9465(98)00015-8

Impact Resistance of Fiber Reinforced Concrete at Subnormal Temperatures

N. Banthia,[a,*] C. Yan[a] & K. Sakai[b]

[a]Department of Civil Engineering, The University of British Columbia, Vancouver, BC, Canada, V6T 1Z4
[b]Materials Section, Civil Engineering Research Institute, Hokkaido Development Bureau, Sapporo, 062 Japan

Abstract

One of the major advantages of reinforcing cement-based materials with randomly distributed fibers is in the improved resistance to dynamic loads. Unfortunately, however, this property of fiber reinforced concrete also happens to be the least understood. While this understanding is critical when designing structures subjected to impact and impulsively applied loads, it is also equally useful while developing better performing fiber reinforced cement composites. In this paper, impact resistance of fiber reinforced concrete was measured using a newly designed drop weight impact machine at two ambient temperatures of 22°C and −50°C. Two hammer approach velocities of 2.42 and 3.43 m/s were investigated. Large, deformed macro-fibers of steel, and fine micro-fibers of steel and carbon were investigated at various fiber volume fractions of up to 2%. Hybrid composites with a combination of macro and micro fibers were also investigated. Results indicate that at a given fiber volume fraction, macro-fibers of steel are far more effective in improving the toughness than micro-fibers, but composites with a hybrid combination of macro and micro fibers are the toughest. Fiber reinforced composites are marginally more impact resistant at a higher hammer velocity, but absorb somewhat diminished amounts of impact energy at a subnormal temperature. Contrary to prevalent belief, however, no particular reduction in the stress-rate sensitivity was observed at subnormal temperatures. © *1998 Elsevier Science Ltd. All rights reserved.*

*To whom correspondence should be addressed. Tel: 604-822-9541; Fax: 604-822-6901; e-mail:banthia@civil.ubc.ca

Keywords: fiber reinforced concrete, micro and macro-fibers, strength, toughness, low temperature.

INTRODUCTION

Fracture in cement-based materials is often believed to be a thermally activated stochastic process.[1,2] This explains the observed sensitivity of cement-based materials to stress-rate and predicts that both strength and fracture toughness will exhibit a strong dependence on the temperature of the environment.

Fiber reinforcement of brittle cement-based materials is one of the most effective ways of improving their resistance to impact, blast, explosion and other forms of dynamic loads when large amounts of energy are suddenly imparted to the structure.[3–8] While we do understand the toughening mechanisms in these composites under statically applied loads, unfortunately, in the case of impact and other dynamic loads, our understanding remains largely qualitative, with little agreement over the exact magnitude of these improvements and with a poor understanding of the underlying mechanisms. Arguably, the root cause of this lack of understanding is the absence of a standardized test technique for conducting impact tests on these cement-based materials.

In addition to frequent occurrences of impact loads, a number of structures such as dams, offshore platforms, bridge piers, etc., may also witness prolonged subnormal climatic temperatures. Data generated so far clearly indicates that moisture plays a very important role in such cases, and sensitivity to temperature is sig-

nificantly amplified at higher moisture contents and at greater water/cement ratios.[9,10] It has also been reported that stress-rate sensitivity is also controlled, to a large extent, by the content and state of moisture in concrete, and cement-based materials are essentially stress-rate insensitive when either in the dry state or at a temperature sufficiently below freezing when moisture is converted to ice in the capillaries.[11,12] Given that these observations have profound implications in the design of structures that are routinely subjected to severe winter climates and frequent impact loads, much further work is necessary to clearly establish the combined influence of climatic harshness and severity of loading on both short term and long term performance of concrete and its fibrous composites. A need also exists to clearly understand the role played by the physical state of the material. The acute need to understand this complex interaction is now well recognized.[13]

EXPERIMENTAL

Materials and mixes

Two matrices of cement mortar (cement: water: silica-fume: sand = 1.0:0.35:0.1:2.0) and concrete (cement: water: silica-fume: sand: coarse aggregate = 1.0:0.35:0.1:2.0:2.0) were reinforced with fibers to produce the composites described in Table 1. The carbon micro-fiber used was pitch-based, 3 mm in length and 18 μm in diameter. The steel micro-fiber was approx. 25×5 μm in section and about 3 mm in average length. The steel macro-fiber chosen was one with crimps along the length, 25 mm in length, 2 mm in width and with a crescent cross section.

Table 1. Composites investigated

Composites	*Matrix*	*Micro-fiber (V_f %)*		*Macro-fiber (V_f %)*
		Carbon	*Steel*	*Steel*
M	Mortar	0	0	0
C	Concrete	0	0	0
MC1	Mortar	1	0	0
MC2	Mortar	2	0	0
MS1	Mortar	0	1	0
MS2	Mortar	0	2	0
CF0.5	Concrete	0	0	1
CF1C1 (hybrid)	Concrete	1	0	1
CF1S1 (hybrid)	Concrete	0	1	1

Specimens

Six beam specimens ($50 \times 50 \times 450$ mm) were cast from each of the mixes given in Table 1 using a high-shear Omni-mixer. Twenty-four hours after casting, the specimens were demoulded and transferred to a moist room at 22 ± 2°C and 95% r.h. for curing. Specimen were cured at least 28 days before testing.

Impact test machine

The impact test machine with the beam specimen is shown in Fig. 1. It is a drop weight type machine with a 10 kg hammer which can be dropped from heights of up to 1.45 m. There is a small pulley and steel wire which can hoist the

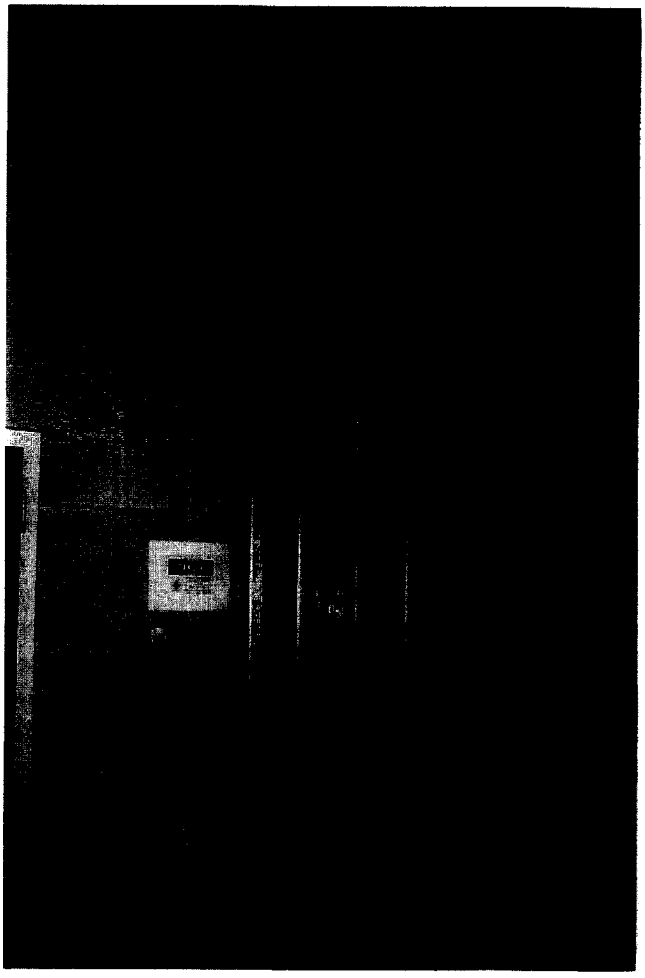

Fig. 1. The Drop Weight Impact Machine with (a) the hammer; (b) the tup; (c) the specimen, and (d) the support.

hammer to the required height, where it is held by a magnetic as well as a mechanical latch. Once both the latches are released, the hammer drops freely on to the beam specimen which rests on two supports 300 mm apart (Fig. 2). The contact end of the hammer (the 'tup') is instrumented with a bolt type load cell which reads the contact load-time pulse between the hammer and the specimen with an accuracy of 20 N. For measurement of specimen displacements, a laser-based, non-contact linear photoelectric sensor (Model MQ-LA-04L-AC, manufactured by Matsushita Electronic Works Ltd) is mounted under the specimen as shown in Fig. 2. The sensor not only features a high resolution (0.01 mm) and a high analog output which can be acquired by a data logger without amplification, but also provides a signal output proportional to the displacement which can then be used in establishing the load vs displacement relationship during a test. For impact tests, the non-contact nature of the sensor is particularly useful because it does not in any way alter the dynamic response of the specimen during an event.

In order to verify if the contactless sensor was capable of accurate measurements, displacements were also measured using two other parallel techniques and the results were compared. The parallel techniques were: first, using accelerometers mounted directly on the specimen output from which could be converted to displacement by twice integrating in the time domain, and second, by using high speed imaging where the use of a high speed camera was made to acquire images at a speed of 1000 frames/s. The results of this comparison are given in Fig. 3. Notice a very good agreement between the three techniques of displacement measurement.

Data analysis

Figure 4 shows some typical hammer-specimen contact load-time pulses recorded during the tests. The peaks in these curves are very high due to the existence of high inertial loads during these impact tests which result essentially from the very high specimen accelerations. To arrive at the actual (and generalized) bending load ($P_b(t)$) on the specimen, one needs to subtract the generalized inertial load ($P_i(t)$) from the measured hammer load ($P_t(t)$). In other words,[14]

$$P_b(t) = P_t(t) - P_i(t) \tag{1}$$

The inertial load, $P_i(t)$, is calculated by using the principle of virtual work and is given by Ref. 14,

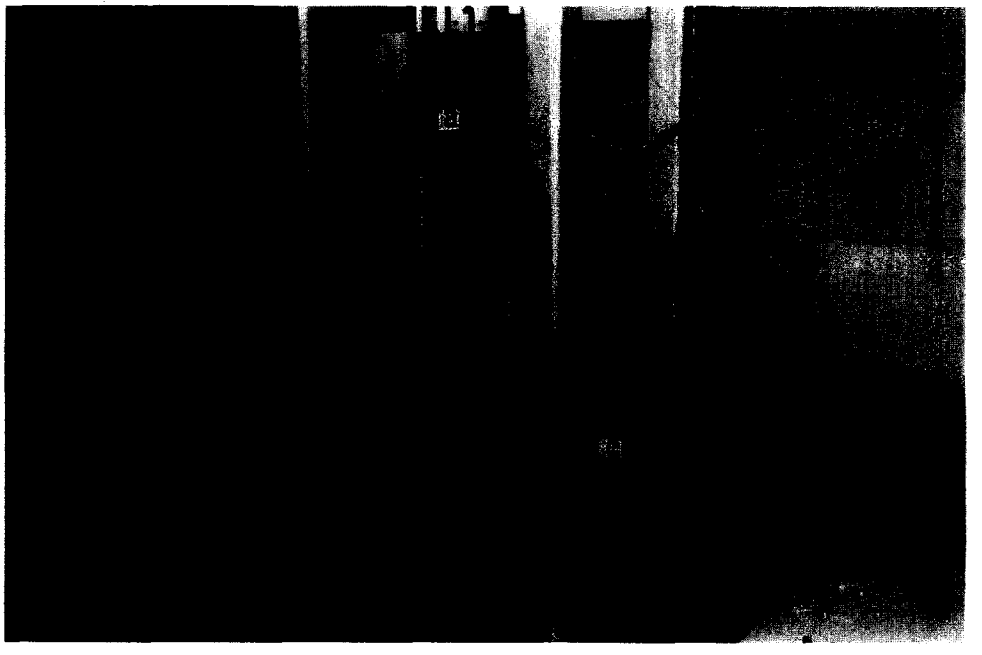

Fig. 2. A close-up of the specimen with (a) the hammer; (b) the tup; (c) the specimen; (d) the support, and (e) contactless infrared displacement transducer.

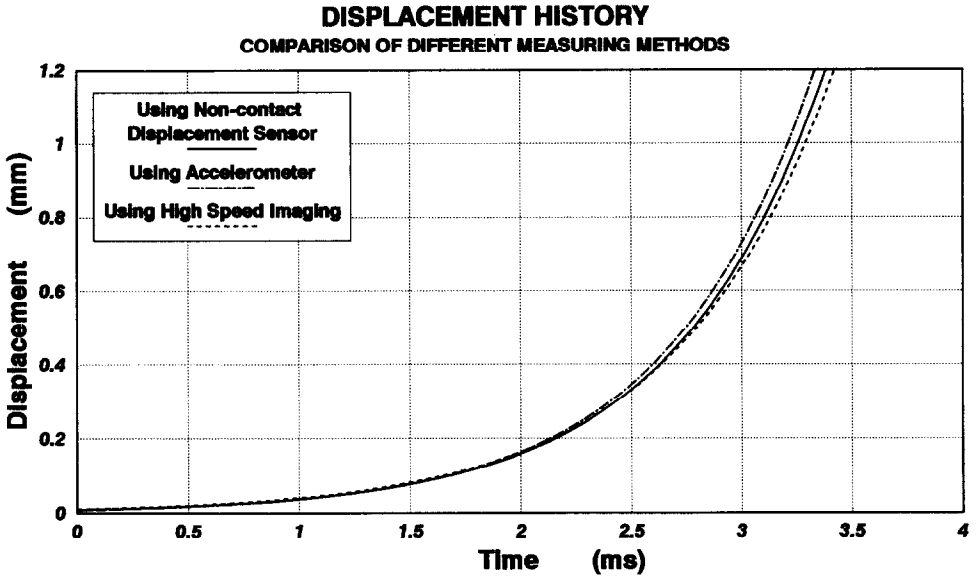

Fig. 3. Comparison of displacement measurements using three different techniques. Note that the displacement measured using the accelerometer signal and high speed imaging compare favorably with those measured using the infrared contactless displacement transducer.

$$P_i(t) = \rho A \ddot{u}_0(t)\left[\frac{l}{3} + \frac{8}{3}\frac{h^3}{l^2}\right] \quad (2)$$

(for the case of linear acceleration distribution) and

$$P_i(t) = \rho A \ddot{u}_0(t)\left[\frac{l}{2} + \frac{2\pi^2 h^3}{3l^2}\right] \quad (3)$$

(for the case of sinusoidal acceleration distribution)where ρ is the mass density of concrete, A

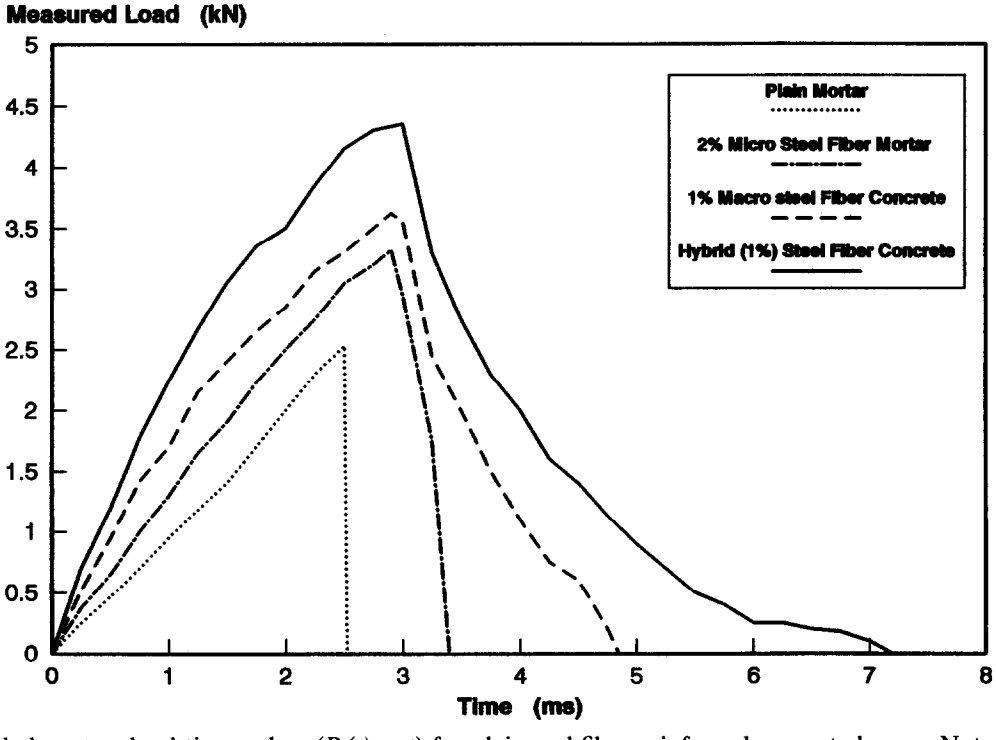

Fig. 4. Recorded contact load-time pulses ($P_i(t)$ vs t) for plain and fiber reinforced concrete beams. Note the larger areas encompassed by beams with fiber reinforcement.

is the cross sectional area of the beam specimen, $\ddot{u}_0(t)$ is the specimen acceleration at the center, h is the beam overhang and l is the test span.

When accelerations are measured directly in a test, as in the previous investigations,[14] $\ddot{u}_0(t)$ can be easily obtained by direct extrapolation. However, when displacements are measured as discrete data points at a certain finite frequency of data acquisition, such as in this study using the contactless laser sensor, calculation of accelerations is not straightforward. Differentiation of the displacement history to obtain the accelerations in such a case can lead to large errors both in velocity and in accelerations. As a solution, a novel method of data representation was adopted, which interpolated between points and defined a function for the curve based on existing points. The following four functions were used to fit the displacement history curves at different stages. The constants a, b, c, d, f, h, k, l, m and n were determined by the least squares method.

$$F(x) = xe^{1-\left(\frac{x}{a}\right)^b} \tag{4}$$

$$F(x) = cx\sin\frac{x}{d} - e^{-fx} + h \tag{5}$$

$$F(x) = k\tanh\left(\frac{x}{l}\right) \tag{6}$$

$$F(t) = mx^k - x^n + px \tag{7}$$

In the above equations x is the argument which in our case is the time, t.

RESULTS AND DISCUSSION

Some contact load-time pulses were previously given in Fig. 4. Notice the influence of fiber reinforcement in terms of encompassing a greater area under the curve ($\int P_t(t)dt$). The energy lost by the hammer during impact is given by Ref. 14:

$$E_h = \frac{1}{2} m_h v_i^2 - \frac{1}{2} m_h \left(v_i - \frac{1}{m_h}\int P_t(t)dt\right)^2 \tag{8}$$

where,

m_h = mass of the hammer

$\int P_t(t)dt$ = contact impulse

v_i = initial velocity of hammer
$= \sqrt{2gh}$

g = earth's gravitational acceleration

h = height of hammer drop

As per eqn (8), a large area under the curve meant an increased loss of hammer energy during an impact and hence a more energy absorbing specimen. Some high speed images of a plain specimen and another specimen with fiber reinforcement are shown in Fig. 5. Notice that for the fiber reinforced specimen, the hammer stays in contact with the specimen for a much longer duration indicating a larger contact impulse, better deformability of the material and a greater transfer of hammer energy.

A study of the acceleration distribution along the length of the beam during an impact test indicated that the same followed a linear distribution, and hence eqn (2) was used to calculate the generalized inertial force and to apply the inertial correction (eqn (1)). In Fig. 6, corrected load–displacement plots based on the contact load vs time pulses of Fig. 4 are given. Notice, again, that fiber reinforcement led to an increase in the area under the curve, which now represents the fracture energy or *impact resistance* for a composite.

In Table 2, the impact resistance of the various composites is given as the calculated fracture energy values under impact. The influence of fiber volume fraction on the impact resistance of various composites is plotted in Figs 7–10. In Fig. 7, data are plotted for mortars with carbon micro-fiber (composites M, MC1 and MC2); in Fig. 8, the same are plotted for mortars with steel micro-fiber (composites M, MS1, MS2); in Fig. 9, concrete with only macro steel fiber and a combination of macro steel and micro carbon are represented (composites C, CF05, CF1, CF1C1); and finally, in Fig. 10, data with concrete reinforced only macro steel fiber and a combination of macro steel and micro steel are plotted (composites C, CF05, CF1, CF1S1). To further understand the data, two sensitivity factors were defined as follows. These sensitivity factors are given in Table 3.

$$\text{Temperature Sensitivity} = \frac{\text{Impact Resistance @ } -50°\text{C}}{\text{Impact Resistance @ } 22°\text{C}} \tag{9}$$

Stress Rate Sensitivity

$$= \frac{\text{Impact Resistance @ 0.60 m Drop}}{\text{Impact Resistance @ 0.30 m Drop}} \quad (10)$$

As evidenced from the data, one can notice that fiber reinforcement is very effective in improving the resistance of cement-based materials to impact loading. The order in which composites exhibited greater and greater impact resistance (fracture energy) were: plain mortar (M), concrete (C), mortar with 1% carbon

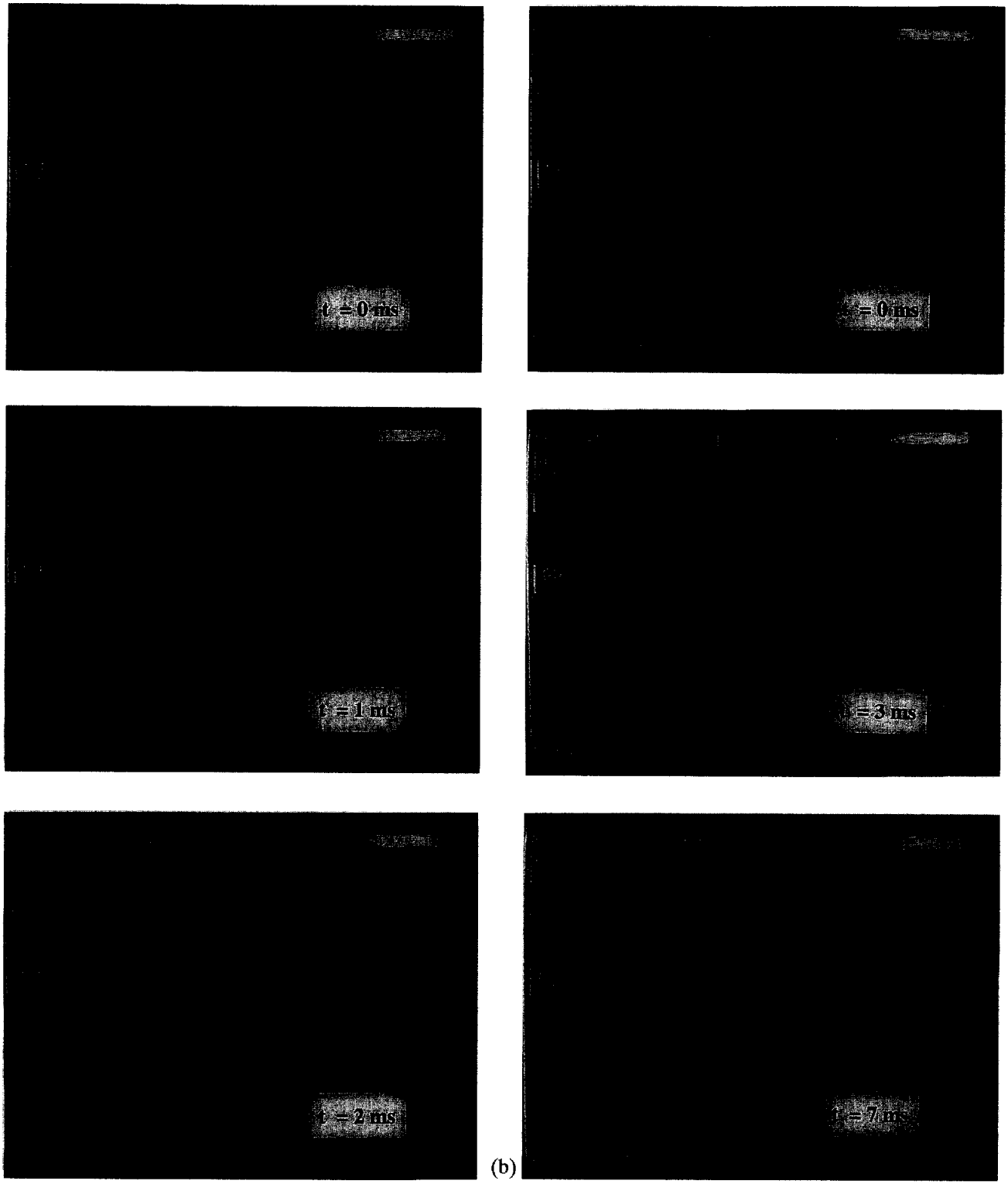

Fig. 5. Typical high speed images acquired during impact on: (a) plain, and (b) fiber reinforced specimen. Notice the longer contact time between the hammer and the specimen for the fiber reinforced specimen (also see Fig. 4).

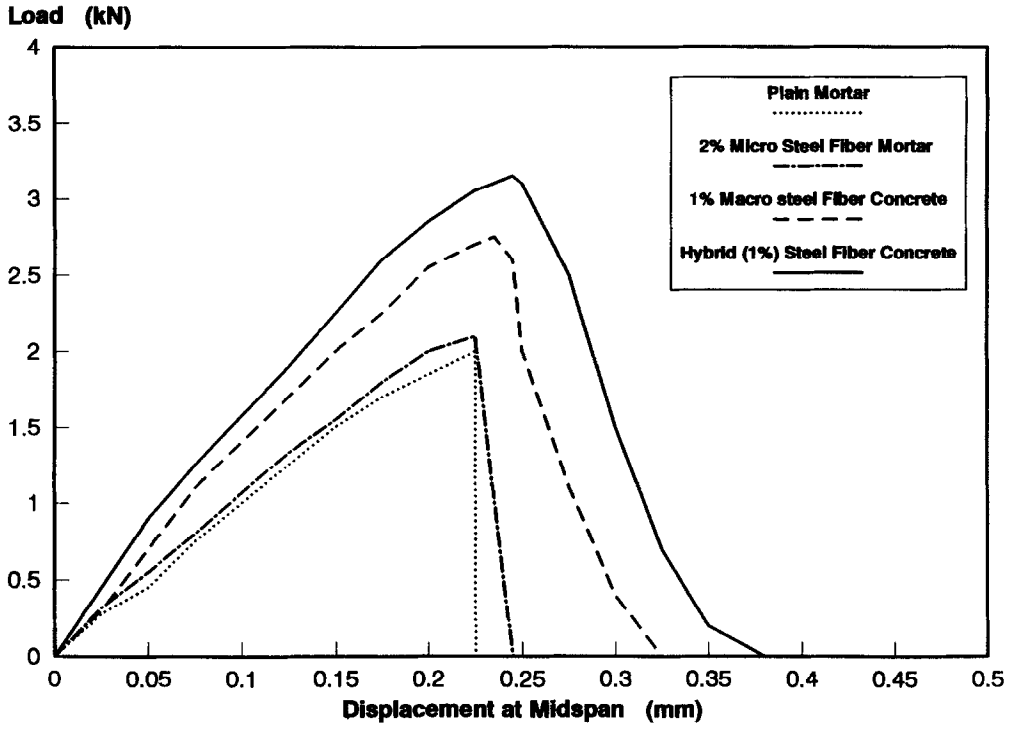

Fig. 6. Typical load vs displacement plots for plain and fiber reinforced concrete specimens. These curves were obtained by applying inertial correction to curves in Fig. 4. Notice the larger area (fracture energy) encompassed by fiber reinforced specimen.

micro-fiber (MC1), mortar with 2% carbon micro-fiber (MC2), mortar with 1% steel micro-fiber (MS1), mortar with 2% steel micro-fiber (MS2), concrete with 0.5% steel macro-fiber (CF05), concrete with 1.0% steel macro-fiber (CF01), concrete with hybrid combination of 1% steel macro-fiber and 1% carbon micro-fiber (CF1C1), and finally, concrete with a hybrid combination of 1% steel macro-fiber and 1% steel micro-fiber (CF1S1). This was true at both normal and low temperatures.

Table 2. Impact resistance (fracture energies) of various composites

Composite	*Drop height (m)*	*Fracture energy (J)*	
		Normal temperature	*Low Temperature*
M	0.3	0.18	0.21
	0.6	0.22	0.24
C	0.3	0.27	0.25
	0.6	0.28	0.25
MC1	0.3	0.29	0.26
	0.6	0.30	0.28
MC2	0.3	0.32	0.29
	0.6	0.33	0.32
MS1	0.3	0.36	0.33
	0.6	0.37	0.35
MS2	0.3	0.38	0.38
	0.6	0.42	0.39
CF0.5	0.3	0.45	0.40
	0.6	0.47	0.43
CF1	0.3	0.49	0.45
	0.6	0.52	0.48
CF1C1	0.3	0.56	0.49
	0.6	0.63	0.51
CF1S1	0.3	0.70	0.58
	0.6	0.87	0.66

The increased absorption of impact energy by concrete over mortar is expected given the possibility of more pronounced micro-cracking (and the resulting quasi-brittle nature of concrete) over mortar. An increase in the impact resistance due to an increase in the volume fraction of fiber is also well expected. When the performance of composites with carbon micro-fiber is compared with those with steel micro-fiber reinforcement, a somewhat inferior performance of the former is noticeable. Although the precise reasons for this are not clear, a similar trend has been previously reported.[15] One can argue that the lower elastic modulus of the pitch-based carbon fiber, its brittle nature and the unfavorable bond characteristics, are partly responsible.

The superior absorption of energy under impact by composites reinforced with large macro-fibers of steel over those reinforced with fine micro-fibers of carbon or steel indicates

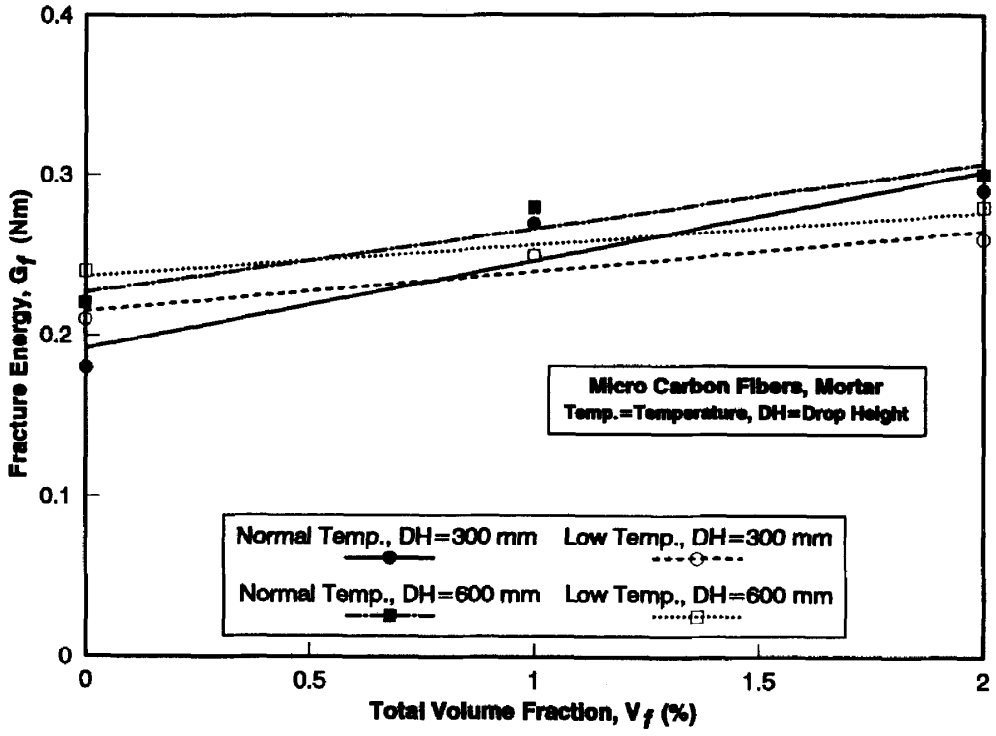

Fig. 7. Impact resistance (fracture energy) of mortars reinforced with carbon micro-fiber (composites M, MC1 and MC2).

that a greater stress transfer capability across a crack at large crack opening displacements is preferable for an improved impact resistance. Micro-fiber reinforcement, by virtue of its fine size and close fiber–fiber spacing, provides an increased strength in tension over the plain matrix[16] and this is generally not possible with large macro-fibers which are farther apart in the

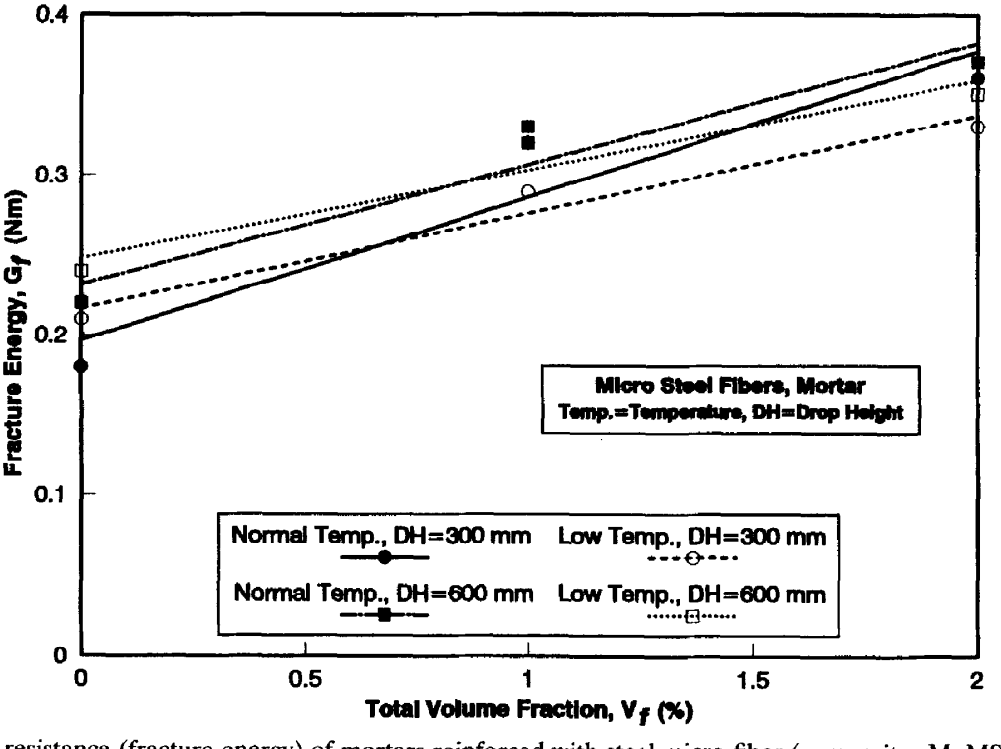

Fig. 8. Impact resistance (fracture energy) of mortars reinforced with steel micro-fiber (composites M, MS1 and MS2).

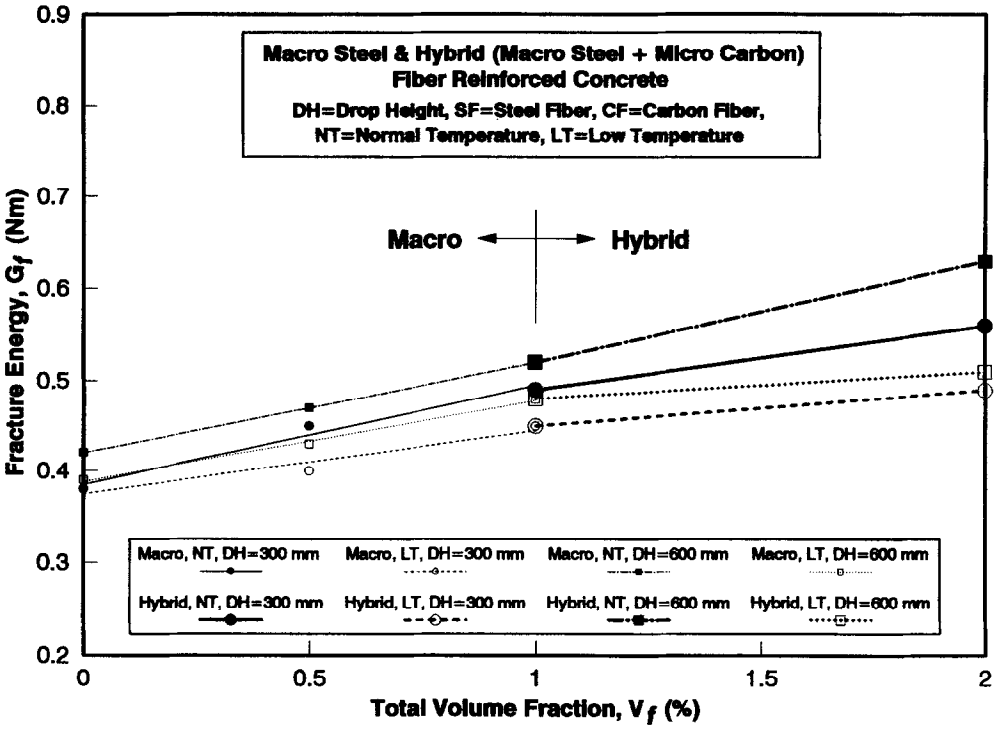

Fig. 9. Impact resistance (fracture energy) of concrete reinforced with either macro steel fiber only (labeled macro) or a combination of macro steel fiber and micro carbon fiber (labeled hybrid) (composites C, CF05, CF1, CF1C1).

matrix. The shorter fiber lengths and the high tensile stresses carried at the occurrence of matrix macrocracking in the micro-fiber reinforced composites results, generally, in a more

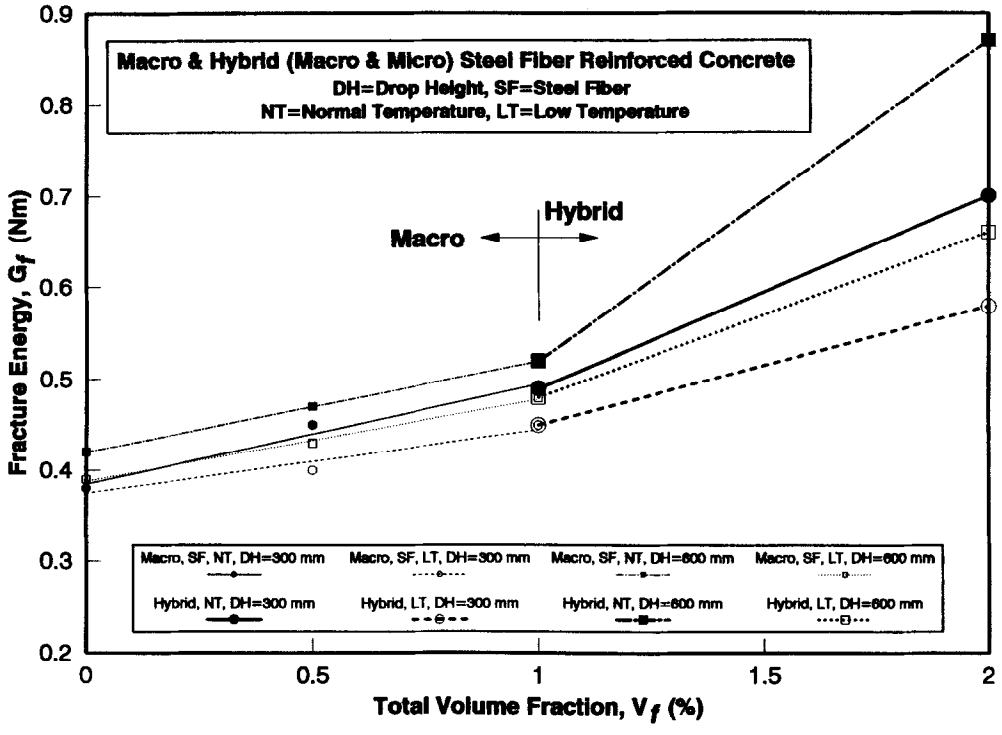

Fig. 10. Impact resistance (fracture energy) of concrete reinforced with either macro steel fiber only (labeled macro) or a combination of macro steel fiber and micro steel fiber (labeled hybrid) (composites C, Cf05, Cf1, Cf1S1).

Table 3. Temperature and stress-rate sensitivity factors

Composite	*Temperature sensitivity*[a]		*Stress-rate sensitivity*[b]	
	@ 0.3 m	*@ 0.6 m*	*@ 22°C*	*@ −50°C*
M	1.16	1.09	1.22	1.14
C	0.92	0.89	1.03	1.00
MC1	0.89	0.93	1.03	1.07
MC2	0.90	0.96	1.03	1.10
MS1	0.91	0.94	1.02	1.06
MS2	1.00	0.92	1.10	1.02
CF05	0.88	0.91	1.04	1.07
CF1	0.91	0.92	1.06	1.06
CF1C1	0.87	0.80	1.13	1.04
CF1S1	0.82	0.75	1.24	1.13

[a]Impact fracture energy @ −50°C/impact fracture energy @ 22°C.
[b]Impact fracture energy @ 0.60 m drop/impact fracture energy @ 0.30 m drop.

brittle post matrix cracking response and an inferior stress-transfer capability at large crack openings.

The synergy observed between the two forms of fiber reinforcements — macro and micro, as in composites CF1C1 and CF1S1, is encouraging. It may be related to an improvement in the bond-slip characteristics between the macro-fibers of steel and the surrounding matrix which, in turn, is reinforced with micro-fibers. Similar observations were reported under static conditions.[17] Given the potential of these hybrid composites, they should be further investigated and the exact mechanisms of the observed synergy should be identified and explored through more fundamental bond-slip tests.

The sensitivity factors given in Table 3 indicate that the composites are marginally less impact resistant at −50°C. This is somewhat in tune with observations made under static conditions in Ref. 18, but contrary those in Ref. 19. To the authors' knowledge no impact data exists for fiber reinforced concrete at low temperatures generated using an instrumented test.

The stress-rate sensitivity of concrete is well documented. The stress-rate sensitivity factors (eqn (10)) reported in Table 3 (based on a comparison between the two drop heights of 0.6 and 0.3 m) indicate that the greater drop height results in a marginal improvement in the impact resistance. This is well expected.[3] What is surprising and somewhat contrary to prevalent belief is that at a low temperature, composites are noted to demonstrate stress-rate sensitivities which are at least comparable to those observed at a normal temperature. In other words, no particular influence of low temperature on the stress-rate sensitivity was noticeable. One must recognize, however, that here, on purpose, the stress-rate sensitivity is not measured with respect to static loading, but between two successive drop heights of the same impact machine. This is done in order to eliminate the influence of machine characteristics on the observed toughness. One must further recognize that in these tests the applied stress-rate varied from composite to composite and as the temperature changed for the same drop height. This is illustrated in Fig. 11, where composite impact strengths (calculated using corrected tup load) are plotted as a function of the time to failure. Notice that, in general, the composites required less time to fail at the lower temperature as compared to the normal temperature. Thus for the same drop height, the composite witnessed a higher stress-rate at the lower temperature.

In a previously published paper,[15] higher specific fracture energy values were reported under impact for micro-fiber reinforced composites similar to those tested here. A number of reasons may be cited for this lack of agreement. In Ref. 15, a pendulum impact machine with a 42.5 kg hammer was used to strike specimens at an approach velocity of 1 m/s in the uniaxial tensile mode. It is possible that among other things, the measured fracture energy in impact for a specimen is not only a function of the hammer mass, hammer velocity, type of machine (pendulum vs drop weight), stiffness of the support system, but also the type of specimen, its boundary conditions and the mode of loading. It has also been argued that, quite possibly, for very brittle materials, a significant portion of the available hammer energy is dissipated in machine vibrations and the higher the machine capacity the greater is the amount of energy lost in this way.[7] A significant amount of additional research is needed before the true influence of machine characteristics on the measured fracture energy values can be understood. This understanding is critical in developing a standardized test.

CONCLUSIONS

1. The use of a contactless, infrared displacement transducer is appropriate for a rational

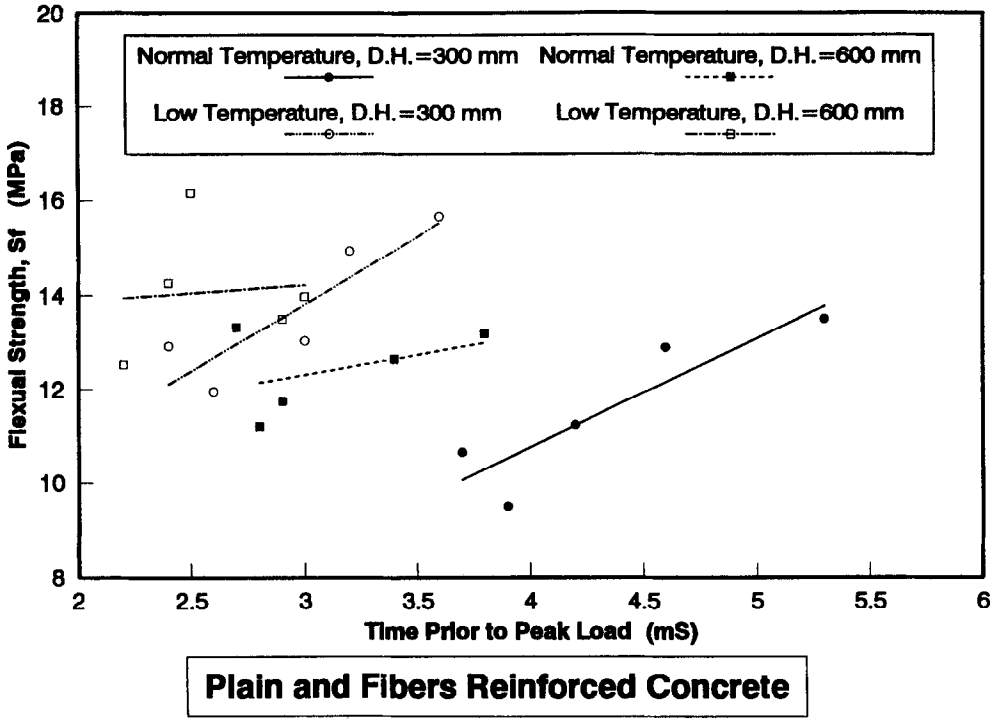

Fig. 11. Measured impact strengths for various composites as a function of the time required for failure. Notice the variation in the applied stress-rate.

analysis of data generated during impact tests on cement-based composites.

2. Fiber reinforcement is a very effective means of improving the impact resistance of cement-based matrices. The order in which composites exhibited greater and greater impact resistance (fracture energy) were: plain mortar, concrete, mortar with 1% carbon micro-fiber, mortar with 2% carbon micro-fiber, mortar with 1% steel micro-fiber, mortar with 2% steel micro-fiber, concrete with 0.5% steel macro-fiber, concrete with 1.0% steel macro-fiber, concrete with hybrid fiber combination of 1% steel macro-fiber and 1% carbon micro-fiber, and finally, concrete with a hybrid fiber combination of 1% steel macro-fiber and 1% steel micro-fiber. This is true at both normal and low temperatures.
3. At a hammer incident velocity of 2.42 m/s, the composites absorbed somewhat lower impact energy than at a hammer incident velocity of 3.43 m/s. Marginal reductions in the impact resistance were also noted at a sub-zero temperature of −50°C as compared to 22°C. No particular difference was observed, however, in the stress-rate sensitivity of these composites at these two temperatures.

ACKNOWLEDGEMENTS

The financial support provided by the Natural Sciences and Engineering Research Council of Canada (NSERC) and the Department of External Affairs and International Trade (DFAIT) under the Japan Science and Technology Fund are gratefully acknowledged.

REFERENCES

1. Bazant, Z. P. & Prat, P. C., Effect of temperature and humidity on fracture energy of concrete. *ACI Materials Journal*, **Jul/Aug** (1988) 262–271.
2. Mihashi, H. & Izumi, M., A stochastic theory for concrete fracture. *Cement and Concrete Research*, **7** (1977) 411–422.
3. Banthia, N., Mindess, S. & Bentur, A., Impact behavior of concrete beams. *Materials and Structures (Paris)*, **20**(119) (1987) 293–302.
4. Suaris, W. & Shah, S. P., Properties of concrete and fiber reinforced concrete subjected to impact loading. *American Society of Civil Engineers, Journal of the Structural Division*, **109**(ST7) (1983) 1717–1741.
5. Zielinski, A. & Reinhardt, H. W., Stress–strain behavior of concrete and mortar at high rates of tensile loading. *Cement and Concrete Research*, **12** (1982) 309–319.
6. Gopalaratnam, V. & Shah, S. P., Properties of steel fiber reinforced concrete subjected to impact loading. *Journal of the American Concrete Institute*, **83**(1) (1986) 117–126.

7. Banthia, N., Mindess, S. & Trottier, J. -F., Impact resistance of steel fiber reinforced concrete. *ACI Materials Journal*, **93**(5) (1996) 472–479.
8. Glinicki, M. A., Toughness of fiber reinforced mortar at high tensile loading rates. *ACI Materials Journal*, **91**(2) (1994) 161–166.
9. Berner, D., Gerwick, B. C. and Polivka, M., Static and cyclic behavior of structural lightweight concrete at cryogenic temperatures, temperature effects on concrete, ed. T. R. Naik. ASTM STP 568, *ASTM*, 1985, 21–37.
10. Rostasy, F. S., Schneider, U. & Wiedmann, G., Behavior of mortar and concrete at extremely low temperatures. *Cement and Concrete Research*, **9** (1979) 365–376.
11. Rossi, P., vanMier, J. G. M., Toutlemonde, F., Le Maou, F. & Boulay, C., Effects of loading rate on the strength of concrete subjected to uniaxial tension. *Materials and Structures*, **27** (1994) 260–264.
12. Kormeling, H. A., *Strain Rate and Temperature Behavior of Steel Fiber Concrete in Tension*. Delft University Press, The Netherlands, 1986.
13. Sakai, K., Banthia, N. & Odd, O. E. (eds), *Concrete under Severe Conditions: Environment and Loading*. E. and F. N. Spon, 1985.
14. Banthia, N., Mindess, S., Bentur, A. & Pigeon, M., Impact testing of concrete using a drop weight impact machine. *Experimental Mechanics*, **29**(2) (1989) 63–69.
15. Banthia, N., Chokri, K., Mindess, S. & Ohama, Y., Fiber reinforced cement-based composites under tensile impact. *Advanced Cement Based Materials*, **1** (1994) 131–141.
16. Banthia, N., Moncef, A. & Sheng, J., Uniaxial tensile response of cement composites reinforced with high volume fractions of steel, carbon and polypropylene micro-fibers. In *Thin Reinforced Concrete Products and Systems*, ed. P. N. Balaguru, ACI SP-146, 1994, pp. 43–68.
17. Banthia, N. & Yan, C., Performance of hybrid fiber reinforced composites with a combination of macro and micro-fibers. Report submitted to Ciment St-Laurent, Quebec, 1995.
18. Banthia, N. & Mani, M., Toughness indices of steel fiber reinforced concrete at sub-zero temperatures. *Cement and Concrete Research*, **23** (1993) 863–873.
19. Staneva, P., Sakai, K., Horiguchi, T. & Banthia, N., Flexural behavior of steel fiber reinforced concrete at low temperatures. Paper presented at ACI Spring Convention, Vancouver, 1992.